

## Microchemical engineering of catalytic reactions

E. Schütz<sup>a</sup>, N. Hartmann<sup>a</sup>, Y. Kevrekidis<sup>b</sup> and R. Imbihl<sup>a</sup>

<sup>a</sup> Institut für Physikalische Chemie und Elektrochemie, Universität Hannover, Callinstrasse 3-3a, D-30167 Hannover, Germany

<sup>b</sup> Department of Chemical Engineering, Princeton University, Princeton, NJ 08544-5263, USA

Received 1 June 1998; accepted 20 July 1998

The catalytic reduction of NO with H<sub>2</sub> or CO and the O<sub>2</sub> + H<sub>2</sub> reaction have been investigated at low pressure ( $p < 10^{-3}$  mbar) on microstructured bimetallic Pt(100)/Rh and Pt(100)/Ti surfaces prepared by lithographic techniques. Photoemission electron microscopy (PEEM) was the spatially resolving technique used. It is shown that diffusional coupling leads to dynamic effects which are size-dependent and thus can be controlled through the design of the surface microstructure. In connection with periodic parameter forcing these dynamic effects can potentially be exploited to improve the yield and selectivity of catalytic reactions.

**Keywords:** chemical waves, surface diffusion, NO reduction, Rh, Pt, composite surfaces, automotive catalytic converter, scanning photoelectron microscopy, photoemission electron microscopy, PEEM

Tailoring catalysts to a desired yield and selectivity lies at the heart of engineering catalysis, and has been one of the main motivations for research in fundamental catalysis and surface science [1,2]. Even today, however, this optimization is done on a purely empirical basis: screening tests narrow down the optimum mixing ratio of the constituents. Bimetallic catalysts provide a prominent example for the synergetic effects present in such composite catalysts [3]. The activity and selectivity optimization obtained there is usually discussed in terms of electronic and geometric effects at the atomic scale. Such interactions, however, are difficult to predict and, moreover, mixing at the atomic level is not easily controllable.

Here we follow a different concept towards a rational design of catalysts. We construct composite surfaces built up by mesoscopic patches of different metals which are coupled through surface transport. Such composite surfaces with features in the 1–100  $\mu\text{m}$  range can be readily prepared by microlithographic techniques [4–6]. By varying the geometry and dimension of the structures one can control the diffusional flow between the differently active metals. Due to this transport coupling nonlinear effects become important. We show in this report that significant dynamic effects arise when a fast diffusing species is present and these effects can be exploited to “steer” a catalytic reaction.

Our model catalysts consist of Pt domains of varying geometry and size surrounded by either (a) a reactive Rh layer or (b) an inert Ti/TiO<sub>2</sub> layer (mimicking the effect of a ceramic support). Their design is motivated by the conventional three-way catalyst (TWC) used in automotive catalytic converters, which contains Pt highly dispersed on a ceramic support to which Rh has been added because of its higher efficiency in dissociating NO [7]. We construct them through a negative photoresist process by deposition of thin layers of either 70 or 500 Å of Rh or of Ti onto a Pt(100)

single crystal surface [6]; the 70 Å thick microstructure consisted of a uniform grid of identical circles; the 500 Å microstructures contained a variety of shapes. Horizontal alloying at the Pt/Rh interface was shown to be restricted to a range  $< 2.5 \mu\text{m}$  [8]. For the 500 Å thickness no change of surface composition due to vertical alloying was detectable. For the thin (70 Å) Rh vertical intermixing resulted in a Rh/Pt alloy with a surface composition Rh : Pt  $\approx 4 : 1$ . The surface of the Ti layer reacts with oxygen so that a TiO<sub>2</sub>/Ti film is generated which was shown to be practically inert under our low pressure reaction conditions.

The dynamical behavior of the reactions we study (the catalytic NO reduction with CO or H<sub>2</sub> as reducing agent as well as the O<sub>2</sub> + H<sub>2</sub> reaction) are well known from a large number of mostly single crystal studies conducted under low pressure conditions [9]. We investigate these reactions in a ultrahigh vacuum (UHV) chamber for  $p < 10^{-4}$  mbar, ensuring strict isothermality. A differentially pumped quadrupole mass spectrometer (QMS) is used to monitor reaction rates. The UHV chamber is equipped with a photoelectron emission microscope (PEEM) in connection with a D<sub>2</sub> discharge lamp as the spatially resolving *in situ* method. PEEM images the local work function with a resolution of ca. 1  $\mu\text{m}$  [10]. Spatially resolved X-ray photoelectron spectroscopy (SXPS, resolution ca. 0.1  $\mu\text{m}$ ) under reaction conditions with the same samples allowed us to chemically identify the different gray levels seen in PEEM and to characterize the metallic substrate [8]. One can essentially distinguish between an oxygen-rich surface which appears dark in the PEEM images and an oxygen-deficient surface which appears bright.

The PEEM images in figure 1 show the titration of an oxygen-saturated Pt(100)/Rh microstructure with hydrogen. The two circles displayed in frame a represent Pt(100) substrate covered by oxygen. They are surrounded by a Rh layer also covered with oxygen. Initially small bright is-

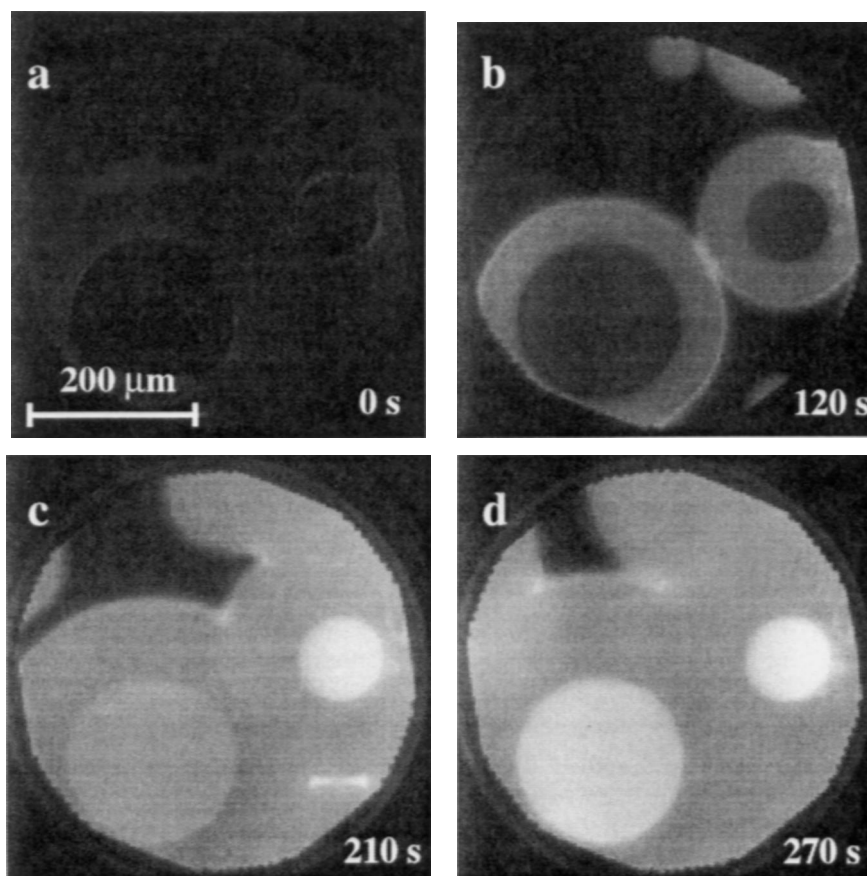


Figure 1. PEEM images showing different stages in the titration of an oxygen-saturated Pt/Rh microstructure with hydrogen at  $p_{\text{H}_2} = 1.5 \times 10^{-7}$  mbar and  $T = 580$  K. Inside the circles the substrate is a Pt(100) surface and the surrounding area is covered with a 500 Å thick Rh film. The bright rings surrounding the Pt domains (frame b) are reaction fronts propagating away from the interface.

lands representing oxygen-freed area are seen to nucleate at the Pt/Rh interfaces (frame a). These islands then coalesce into closed rings which propagate outward from the Pt/Rh boundaries with a constant velocity of  $0.45 \mu\text{m/s}$  forming perfectly circular reaction fronts (frame b), leaving behind an oxygen-freed Rh layer. Only in the final stage of this process is the remaining oxygen inside the Pt domains completely reacted off, apparently spatially uniformly. The small domain reacts first and the larger one follows with a delay of ca. 60 s (frames c and d). This mesoscopic size effect can be rationalized in a simple way. Hydrogen adsorbing on the oxygen-freed Rh area will diffuse back into the Pt circles, at a rate roughly proportional to their perimeter, and accelerate the reactive removal of oxygen there. Since the oxygen to be reacted off is proportional to the area of the circle, the diffusional contribution will vary as  $1/r$ . Therefore, smaller Pt circles should react faster, in agreement with our observations. Notice that the surface diffusion of atomic hydrogen must be fast because the transition to the oxygen-free state inside the Pt circle proceeds spatially uniformly without an apparent reaction front [11].

We also investigated the influence of differently active surroundings on the reactivity of an adsorbed layer. In the reaction  $\text{NO} + \text{CO} \rightarrow (1/2)\text{N}_2 + \text{CO}_2$ , at 300 K the surface is in its inactive state, fully covered by molecu-

lar NO/CO adsorbate; the reactivity of the Pt(100) surface at low temperature is limited by the availability of vacant sites required for the dissociation of NO [12,13]. Upon heating, however, a sharp transition ("surface explosion") to the reactive state occurs as the combined NO/CO coverage falls below 0.5, triggering an autocatalytic increase in the number of vacant sites. On an extended Pt(100) surface this occurs via reaction fronts nucleating at some defects (scratches, etc.); on Pt(100)/Rh the reaction fronts always develop at the Pt/Rh interface.

A plot of the ignition temperature,  $T_{\text{ign}}$ , for Pt domains surrounded by Rh in figure 2 shows an inverse dependence of reactivity on the domain radius,  $r$ . Pt domains surrounded by a freshly cleaned Ti/TiO<sub>2</sub> layer (after brief sputtering) show precisely the opposite trend. No dependence of  $T_{\text{ign}}$  on the domain radius is seen after the Ti/TiO<sub>2</sub> layer had been in use for some time. Rh is more active in the NO + CO reaction than Pt and therefore an outflow of both, NO and CO, across the Pt/Rh boundary will occur. This decreases the NO/CO coverage in the Pt domain thus reducing its ignition temperature. This effect will again be strongest for small domains. For an inert (zero flux) boundary one would expect  $T_{\text{ign}}$  to be independent of  $r$ ; this is what is seen in the Ti/TiO<sub>2</sub> experiment. The surprising increase of  $T_{\text{ign}}$  with decreasing radius for a freshly

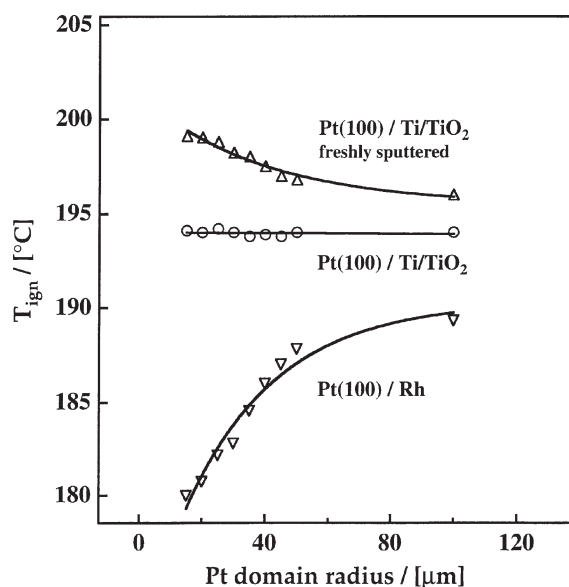


Figure 2. Influence of the boundary conditions and of the domain size on the ignition of a molecularly adsorbed NO/CO layer on Pt(100). The plot shows the dependence of the ignition temperature,  $T_{\text{ign}}$ , on the domain radius for circular Pt(100) domains surrounded either by a reactive 500 Å Rh layer or by an unreactive 500 Å Ti/TiO<sub>2</sub> layer. The samples were slowly heated up in a NO/CO atmosphere starting from 300 K. Experimental conditions:  $p_{\text{NO}} = 1.2 \times 10^{-5}$  mbar,  $p_{\text{CO}} = 0.9 \times 10^{-5}$  mbar,  $T = 459$  K, heating rate 0.1 K/s.

sputtered Ti/TiO<sub>2</sub> layer suggests that such a boundary acts as a supplier of NO/CO.

The last examples show that domain reactivity can be modified through design of the chemical composition and the geometry of the domain boundaries. In order to demonstrate that it is possible to steer a catalytic reaction by controlling diffusional coupling (here through chemical waves), we need to show effects on the global reaction rate, representing the integral over the whole reacting surface area. The different patterns seen in PEEM have to be related to overall reaction rates and the behaviour should be sustained and not transient. For this purpose we designed a Pt/70 Å thickness Rh microstructure on which the entire surface ( $5 \times 5$  mm) was uniformly covered with Pt circles of 100 μm diameter. Due to the enhanced reactivity of the Pt/Rh interface [14], the waves nucleate preferentially there. To establish sustained chemical waves taking advantage of this enhanced interface reactivity, we apply a periodic modulation of the partial pressure of one of the reactants ( $p_{\text{H}_2}$ ) in a NO/H<sub>2</sub> mixture.

In the first experiment we study the coupling between Pt domains and their Rh/Pt alloy surroundings via reaction fronts. We increase  $p_{\text{H}_2}$  slowly up to the point where a reaction front is ignited and then keep  $p_{\text{H}_2}$  constant. Figure 3 displays the propagation of the reaction front on the oxygen-covered Rh/Pt layer as it comes into contact with

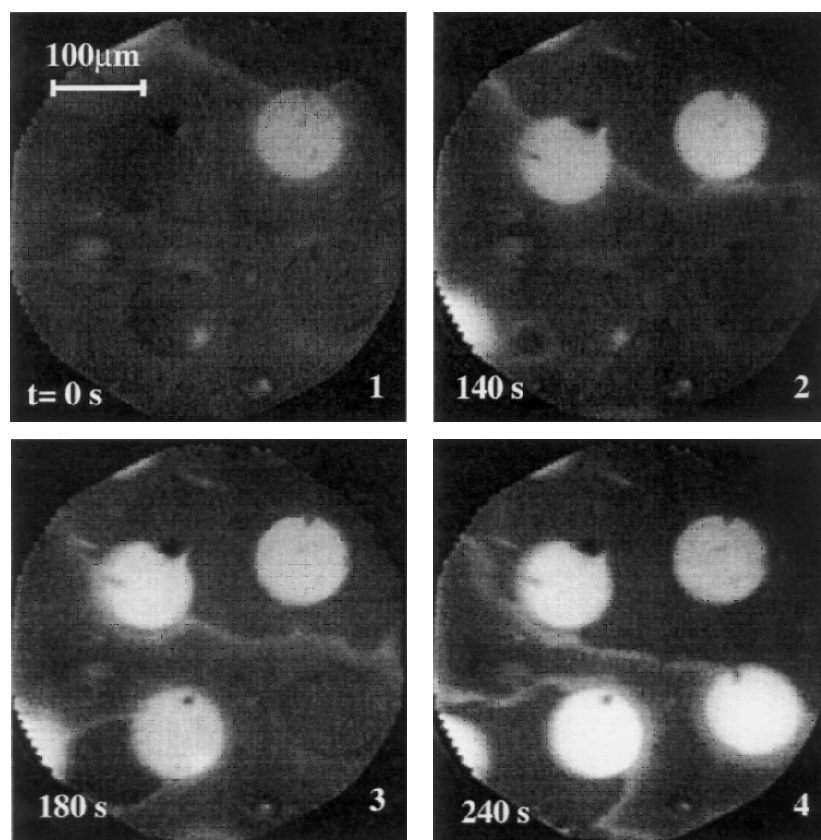


Figure 3. Triggering of the reactive removal of oxygen inside the Pt circles as a reduction front advancing on the Rh/Pt layer gets into contact with the circles. The four circles visible in the frames are Pt(100) domains surrounded by a partially oxidized 70 Å thick Rh/Pt layer with a surface composition Rh:Pt  $\approx$  4:1. Experimental conditions:  $p_{\text{NO}} = 1 \times 10^{-7}$  mbar,  $p_{\text{H}_2} = 3 \times 10^{-7}$  mbar,  $T = 563$  K.

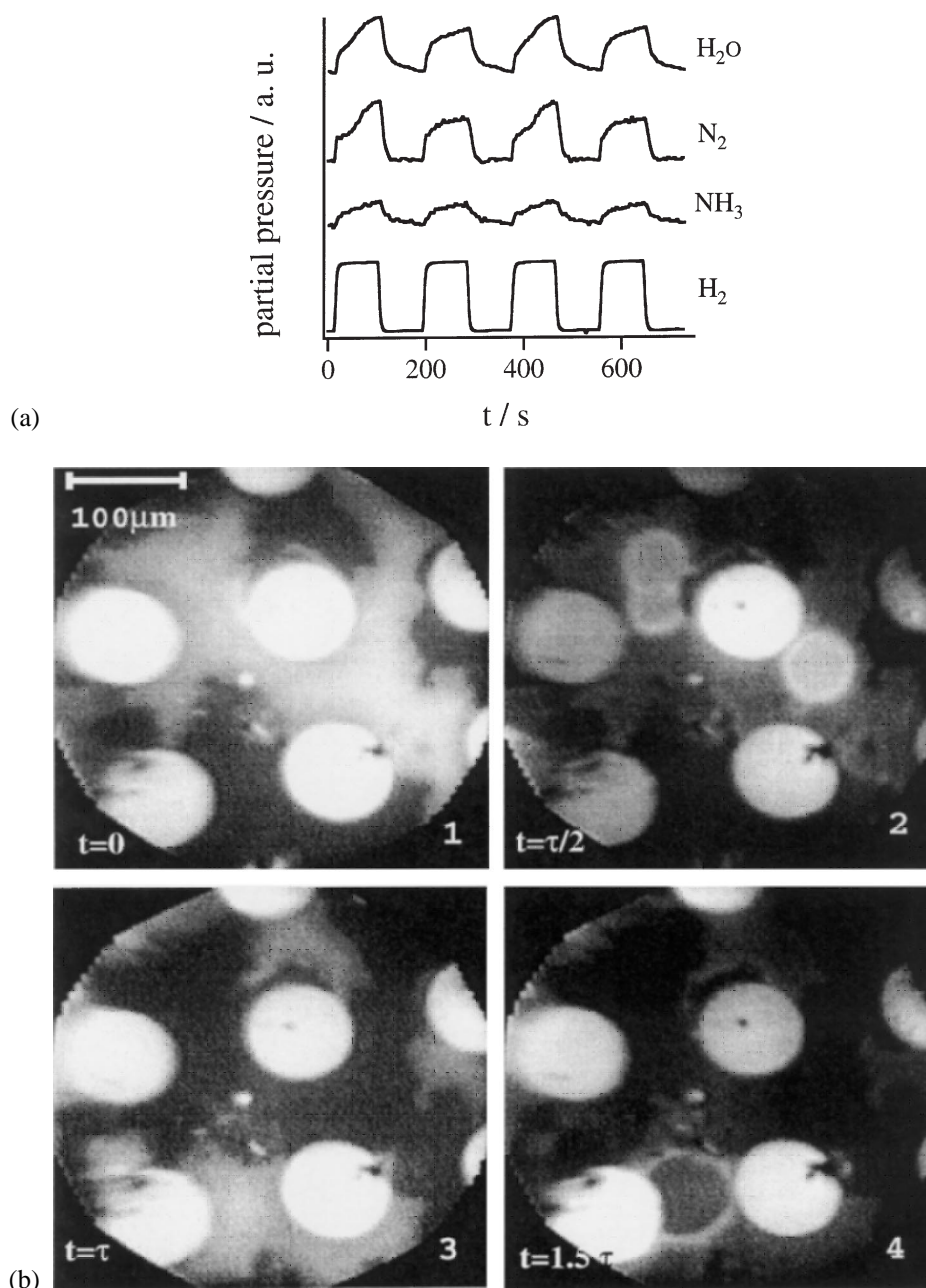


Figure 4. Subharmonic resonance in the periodic forcing of the  $NO + H_2$  reaction catalyzed by a Pt(100)/Rh microstructure (see legend of figure 3). Experimental conditions:  $p_{NO} = 1 \times 10^{-6}$  mbar,  $p_{H_2}(\max) = 2 \times 10^{-5}$  mbar,  $p_{H_2}(\min) < 2 \times 10^{-7}$  mbar,  $T = 558$  K. (a) Modulated partial pressure of hydrogen and resulting variation of the  $H_2O$ ,  $N_2$  and  $NH_3$  production rates. (b) PEEM images showing the origin of the period two seen in (a). The four images were taken separated by half a modulation period ( $\tau = 182$  s) starting with  $p_{H_2}$  at its minimum.

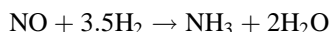
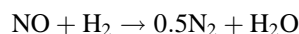
Pt circles which are likewise covered with oxygen. The front initiates a transition from an unreactive state (gray area ahead of the front) to a reactive state (dark area behind the front). Due to alloying the usual correlation – high oxygen coverage/low PEEM intensity – is no longer valid here. The dark reactive area of the Rh/Pt layer exhibits a substantial coverage of atomic nitrogen and it is associated with a lower oxygen coverage than the unreactive gray area which contains an oxidic species [8]. The first frame in figure 3 (0 s) shows that as soon as the reduction front touches the Pt circle in the upper right corner this circle rapidly turns bright, i.e., the oxygen in-

side the Pt circle is reacted away. The remaining circles turn sequentially bright as they get contacted by the front.

The interpretation of this “switching” effect is straightforward. A high oxygen coverage inside the Pt circles inhibits the dissociative chemisorption of hydrogen thus protecting the oxygen on Pt against reactive removal. In mathematical terms, the bistable system  $Pt/NO + H_2$  is in its low activity state. Adsorbed, already dissociated hydrogen atoms from the reduction zone can, however, diffuse inside the Pt circle where they react off with adsorbed oxygen. The vacant sites for dissociative  $H_2$  chemisorp-

tion which are thus created trigger the transition to the oxygen-free state of the bistable system. We see that the fast diffusion of hydrogen can signal an almost instantaneous switching in the dynamic state of the Pt domains.

Catalytic reduction of NO with H<sub>2</sub> on Pt/Rh involves two competing reaction pathways leading to N<sub>2</sub> and NH<sub>3</sub> (N<sub>2</sub>O is formed only to a minor extent at low *p*):



When we periodically modulate *p*<sub>H<sub>2</sub></sub> the yield and selectivity vary depending on the forcing and reaction parameters. In the following we try to establish a connection between the integral reaction rate and selectivity and the nucleation of chemical waves; the latter is controlled by the *p*<sub>H<sub>2</sub></sub> modulation and by the relative reactivity of the domains and their interface.

We first take a look at a subharmonic resonance (the period of the rate is twice that of the forcing) shown in figure 4(a) which occurs during such a forcing experiment. The corresponding PEEM images displayed in figure 4(b) reveal very clearly the nature of the period two. At *t* = 0, at low *p*<sub>H<sub>2</sub></sub>, the Rh/Pt layer is in an inhomogeneous state with the inactive high oxygen coverage (gray) area and the active low oxygen coverage (dark) area in equal proportions. As *p*<sub>H<sub>2</sub></sub> is raised to  $9 \times 10^{-6}$  mbar circular reduction fronts nucleate on the gray area (*t* =  $\tau/2$ ) and at the end of the first modulation period (*t* =  $\tau$ ) the initial intensity distribution on the Rh/Pt layer has been reversed, i.e., the initially gray area has turned black and vice versa. When *p*<sub>H<sub>2</sub></sub> is now raised again reduction fronts nucleate again on the gray area (frame 4) and at the end of the second modulation period the initial state is restored. The reason for the period two is evidently that the modulation of *p*<sub>H<sub>2</sub></sub> is too fast compared to the time scale of oxidation and reduction in the Rh/Pt layer. The latter proceeds via a propagating reaction front and, therefore, the surface becomes inhomogeneous for too fast a modulation.

When we choose a slower modulation frequency the reduction fronts nucleate preferentially at the Pt/Rh interface. Due to this controlled nucleation the reaction fronts will completely transform the surface from the oxidized state of the Rh/Pt layer to the reduced one over a single period of the forcing. The net result is that integrated over space and time the surface becomes more active and the yield of N<sub>2</sub> and NH<sub>3</sub> increases with decreasing modulation frequency as demonstrated by figure 5. It is worth noting that the selectivity towards N<sub>2</sub> increases in the same direction.

The effect of nanoscale and microscale structures on catalytic reactions has already been investigated by several groups [4,15–17], but these experiments have been conducted at high pressure (*p* > 1 mbar) and therefore no *in situ* observations were possible relating the changes in catalytic activity to dynamic surface processes. We have

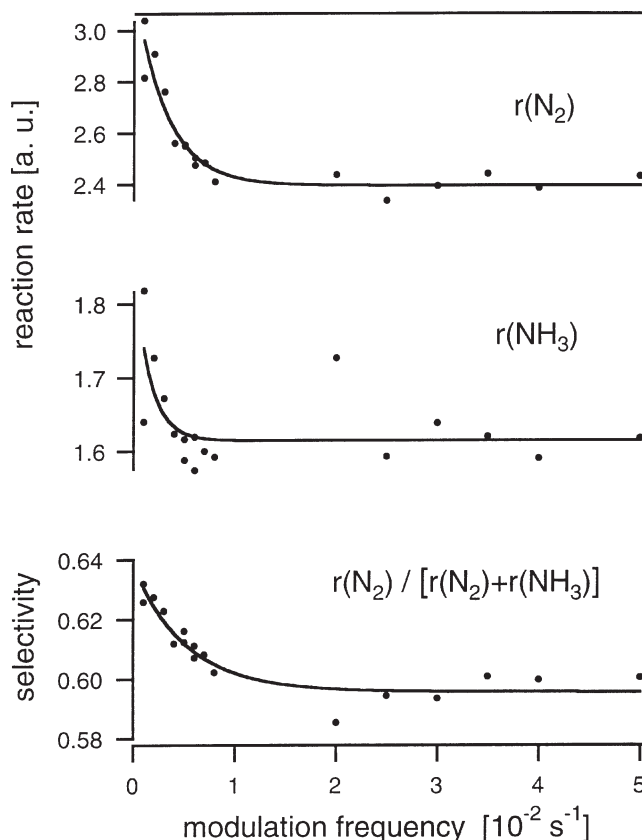


Figure 5. Dependence of the product yields for N<sub>2</sub> and NH<sub>3</sub> and of the selectivity on the modulation period for the forcing experiments displayed in figure 4.

seen that a fast diffusing species like hydrogen can lead to dynamical coupling effects over mesoscopic distances – effects which can also decisively affect the macroscopic behavior of a catalyst. In this report controlled front nucleation at domain interfaces as well as the switching of domain reactivities triggered by their surroundings were demonstrated. Since these effects are size dependent, they can be controlled by appropriately designed composite surfaces. In particular, the very fast diffusion of hydrogen opens an avenue towards a microchemical engineering of catalysis by designing surfaces with sinks and sources for the hydrogen. While the economic use of such catalysts may still lie far ahead in the future, the study of such systems provides us with the unique opportunity to systematically investigate dynamic effects in catalysis – a possibility which would be rather difficult to realize with real catalysts.

## Acknowledgement

This work was financially supported by the BMBF (FRG) and the NSF (USA). The authors thank M. Graham for original discussions and M. Lange for the preparation of the catalysts.

## References

- [1] J.M. Thomas and W.J. Thomas, *Principles and Practice of Heterogeneous Catalysis* (VCH, Weinheim, 1997).
- [2] G.A. Somorjai, *Principles of Surface Chemistry and Catalysis* (Wiley, New York, 1994).
- [3] J.H. Sinfelt, *Bimetallic Catalysts* (Wiley, New York, 1983); C.T. Campbell, *Ann. Rev. Phys. Chem.* 41 (1990) 775.
- [4] I. Zuburtikudis and H. Saltsburg, *Science* 258 (1992) 1337.
- [5] K. Asakura, J. Lauterbach, H.H. Rotermund and G. Ertl, *J. Chem. Phys.* 102 (1995) 8175.
- [6] M.D. Graham, Y.G. Kevrekidis, K. Asakura, J. Lauterbach, K. Krischer, H.H. Rotermund and G. Ertl, *Science* 264 (1994) 80; M.D. Graham, M. Bär, Y.G. Kevrekidis, K. Asakura, J. Lauterbach, H.H. Rotermund and G. Ertl, *Phys. Rev. E* 52 (1995) 76.
- [7] K.C. Taylor, in: *Automobile Catalytic Converters* (Springer, Berlin, 1984).
- [8] F. Esch, S. Günther, E. Schütz, M. Marsi, M. Kiskinova, Y.G. Kevrekidis and R. Imbihl, in preparation.
- [9] R. Imbihl and G. Ertl, *Chem. Rev.* 95 (1995) 697.
- [10] W. Engel, M.E. Kordes, H.H. Rotermund, S. Kubala and A. von Oertzen, *Ultramicroscopy* 36 (1991) 148.
- [11] E.G. Seebauer and C.E. Allen, *Progr. Surf. Sci.* 49 (1995) 265.
- [12] M. Lesley and L.D. Schmidt, *Surf. Sci.* 155 (1985) 215.
- [13] T. Fink, J.-P. Dath, R. Imbihl and G. Ertl, *J. Chem. Phys.* 95 (1991) 2109; G. Voser, P.A. Thiel and R. Imbihl, *J. Phys. Chem.* 98 (1993) 2148.
- [14] H. Hirano, T. Yamada, K.I. Tanaka, J. Siera, P. Cobden and B.E. Nieuwenhuys, *Surf. Sci.* 262 (1992) 97.
- [15] A.C. Krauth, K.H. Lee, G.H. Bernstein and E.E. Wolf, *Catal. Lett.* 27 (1994) 43.
- [16] P.W. Jacobs, S.J. Wind, F.H. Ribeiro and G.A. Somorjai, *Surf. Sci.* 372 (1997) L249.
- [17] M. Liauw, J. Ning and D. Luss, *J. Chem. Phys.* 104 (1996) 5657.